IOP Publishing Journal of Physics B: Atomic, Molecular and Optical Physics

J. Phys. B: At. Mol. Opt. Phys. **40** (2007) 1907–1915 doi:10.1088/0953-4075/40/10/023

Narrow bandwidth electromagnetically induced transparency in optically trapped atoms

Bernd Kaltenhäuser[1], Harald Kübler[1], Andreas Chromik[1], Jürgen Stuhler[1], Tilman Pfau[1] and Atac Imamoglu[2]

[1] 5. Physikalisches Institut, Universität Stuttgart, 70550 Stuttgart, Germany[3]
[2] Institute of Quantum Electronics, ETH-Zürich, 8093 Zürich, Switzerland

E-mail: b.kaltenhaeuser@physik.uni-stuttgart.de and t.pfau@physik.uni-stuttgart.de

Received 12 March 2007, in final form 13 March 2007
Published 1 May 2007
Online at stacks.iop.org/JPhysB/40/1907

Abstract

We demonstrate electromagnetically induced transparency (EIT) in a sample of rubidium atoms, trapped in an optical dipole trap. Mixing a small amount of σ^--polarized light to the weak σ^+-polarized probe pulses, we are able to measure the absorptive and dispersive properties of the atomic medium at the same time. Features as small as 4 kHz have been detected on an absorption line with 20 MHz line width.

(Some figures in this article are in colour only in the electronic version)

1. Introduction

Electromagnetically induced transparency allows for the elimination of absorption in an otherwise opaque medium [1]. Here, an additional laser is used to modify the absorptive and dispersive properties of the sample. On the level of single excitations, the corresponding collective excitations can be described as a quasi-particle, the so-called dark-state polariton [2]. Recently, the particle nature of dark-state polaritons has been experimentally demonstrated [3].

In quantum information processing, photons can be used as robust information carriers [4]. Several experiments have used the concept of dark-state polaritons to store photonic information in cold atoms [5] and vapour cells [6]. Furthermore, as a step towards storage in a solid, electromagnetically induced transparency (EIT) has been demonstrated in a room-temperature solid [7]. It has also been shown theoretically that EIT in atomic ensembles can be used to enhance the possibilities of long-distance quantum communication [8].

Here, we report on the first experimental demonstration of EIT in an optical dipole trap. Contrary to magneto-optical and magnetic traps, our setup allows for arbitrary magnetic fields,

[3] http://www.pi5.uni-stuttgart.de.

particularly for a high and homogenous offset field. This offset field can be used to address different magnetic substates of the medium. Furthermore, the storage time in a magnetic trap is limited by the inhomogeneous magnetic broadening. Long storage times for photonic information require both a high degree of transmission and narrow bandwidth in the EIT signal. We have measured 4 kHz features in the EIT response on an absorption line that is broadened by the Stark shift of the dipole trap to 20 MHz. This is an important step towards long storage times of quantum information in an atomic ensemble and the investigation of trapped dark-state polaritons. For a more dense sample, we expect a high degree of transmission at the same linewidth. Therefore, optically trapped atoms are well suited for photon storage experiments.

2. Experimental setup

To prepare an absorbing medium of trapped atoms, we first capture 2×10^9 Rb-87 atoms in a magneto-optical trap. The beam diameters are 10 mm, with a power of 20 mW in each beam. The overlapped repump laser beams have an intensity of 1 mW each.

Afterwards, we apply a dark-MOT phase (DM) for 25 ms to ensure an efficient transfer of the atoms to the dipole trap. For the DM, we ramp up the magnetic gradient field from 13.7 to 18 G cm^{-1}, detune the MOT lasers to -100 MHz from resonance of the $F = 2 \longrightarrow F' = 3$ transition on the D2 line at 780.247 nm and lower the repump laser power to 1%. After the DM, we have 9×10^8 atoms at a temperature of 38 μK and a density of 10^{12} atoms cm^{-3} left.

The crossed CO_2-laser dipole trap (DT) is turned on during the loading steps described above. After switching off the DM and additional 80 ms thermalization time we capture 3×10^7 atoms at a density of 2×10^{11} atoms cm^{-3} in the DT. The widths of the cloud are $\sigma_y \approx \sigma_z = 126$ μm and $\sigma_x = 272$ μm. Due to optical pumping, the atoms are distributed over the five magnetic substates of the $5S_{1/2}, F = 2$ ground state. Because the potential of the DT is much steeper than the one of the DM, the cloud heats up to a temperature of 110 μK. The cloud provides a medium with an optical density up to 0.76 for a single Zeeman component on resonance. Due to a relatively high pressure in the chamber, the lifetime in the trap is 770 ms.

For the EIT measurements, a magnetic offset field of 129.7 G is applied parallel to the laser beam propagation. At this field strength, the magnetic substates of the $5S_{1/2}$ ground state can be addressed individually. This allows us to perform the EIT measurement only between the $5S_{1/2}, F = 2, m_F = -1$ and $5S_{1/2}, F = 1, m_F = +1$ substates. At the field strength of 129.7 G, their Zeeman shifts are -87.07 MHz and -94.34 MHz, respectively, while (negligible) one of the excited states is 4.4 MHz. We use a Raman laser system to address these transitions, which are shown in figure 1. The relative stability between the two laser frequencies is better than 0.85 Hz.

The setup for the EIT measurements is shown in figure 2. For revealing the dispersive properties of the medium, the first $\lambda/4$ plate is turned to mix σ^--polarized light to the probe beam. The electric field admixture is denoted with a. This results in an intensity admixture a^2, which was used as one of the fitting parameters. The second $\lambda/4$ plate compensates this effect and mixes both polarizations back to linearly polarized light, which is then measured beyond the second polarizing beamsplitter. This causes the two polarizations to interfere. A similar method has recently been demonstrated with a vapour cell [9, 10].

Due to the large Zeeman shift of the magnetic substates, the Raman condition is not fulfilled for the wrong polarizations and thus the admixture in the coupling beam can be neglected.

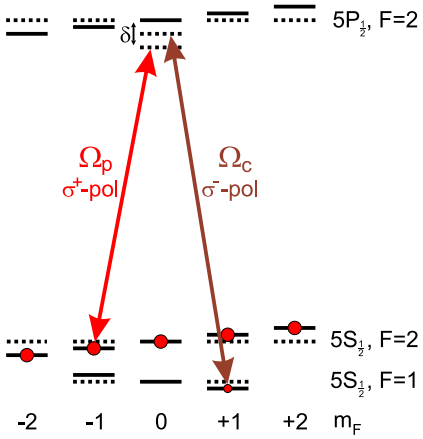

Figure 1. Level scheme of the EIT transition. The probe laser couples to the $5S_{1/2}$, $F = 2, m_F = -1 \longleftrightarrow 5P_{1/2}$, $F = 2, m_F = 0$ transition, the coupling laser to the $5S_{1/2}$, $F = 1, m_F = +1 \longleftrightarrow 5P_{1/2}$, $F = 2, m_F = 0$ transition. The detuning of the coupling laser corresponds to the differential quadratic Zeeman shift of the ground states. The two-photon resonance is met when the probe laser detuning reaches the quadratic Zeeman shift of ~ -7.27 MHz.

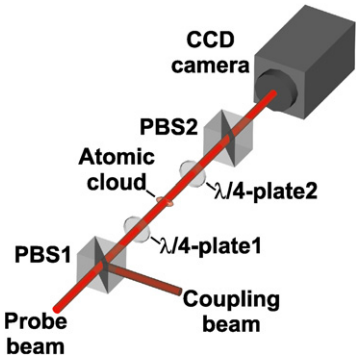

Figure 2. Setup for the experiment: the probe and the coupling laser are overlapped in a polarizing beamsplitter (PBS). With the following $\lambda/4$ plate the polarization of the pulses are adjusted before they enter the cloud. With the second $\lambda/4$-plate the polarizations are turned again to separate the probe from the coupling beam in the following polarizing beamsplitter. Due to lenses (not shown in the picture), the cloud is imaged onto a high-efficiency CCD camera.

3. Theory

As described above, the first $\lambda/4$ plate mixes a relative intensity a^2 of σ^- polarization into the otherwise σ^+-polarized probe beam. Due to birefringence in the optical viewports of the vacuum chamber, the σ^--polarized beam collects an additional phase ϕ relative to the σ^+-polarized beam. The total electric field acting on the atoms can then be described via

$$\begin{aligned} |E_{\text{in}}|^2 &= |E_{\text{in},\sigma^+} + E_{\text{in},\sigma^-}|^2 \\ &= |(1-a)E_0 + aE_0 \exp\{\mathrm{i}\phi\}|^2 \\ &= E_0^2(1 - 2a + 2a^2 + 2a(1-a)\cos\phi), \end{aligned} \tag{1}$$

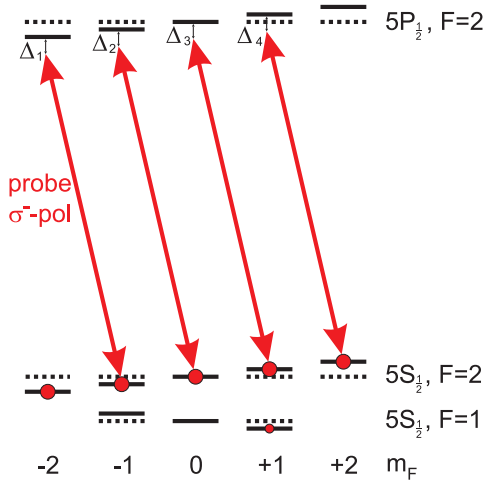

Figure 3. Level scheme for the σ^--polarized component of the probe light: the detunings of the respective transitions j are marked as Δ_j.

where E_0 denotes the electric field amplitude. When we tune the coupling laser to resonance, the single-photon and two-photon detuning of the probe laser become identical and the susceptibility for the σ^+-polarized probe laser is given by [11]

$$\chi^{(+)} = \frac{|\mu|^2\varrho}{\epsilon_0\hbar}\left[\frac{4\delta\left(\Omega_c^2 - 4\delta^2 - \gamma^2\right)}{\left|\Omega_c^2 + (\Gamma + \mathrm{i}2\delta)(\gamma + \mathrm{i}2\delta)\right|^2} + \mathrm{i}\frac{8\delta^2\Gamma + 2\gamma\left(\Omega_c^2 + \gamma\Gamma\right)}{\left|\Omega_c^2 + (\Gamma + \mathrm{i}2\delta)(\gamma + \mathrm{i}2\delta)\right|^2}\right]. \tag{2}$$

To derive this equation, we have also assumed that the relevant atomic population stays mainly in the initial $5S_{1/2}, F = 2, m_F = -1$ state. This is fulfilled, if a strong-coupling laser or weak-probe pulses ($N_{\text{photons}} \ll N_{\text{atoms}}$) are used. Here, δ is the probe laser detuning, Ω_c is the Rabi frequency of the coupling laser, Γ is the spontaneous emission rate between the excited state and the respective ground state, γ is the collisional decay rate between the two ground states and $|\mu|$ is the dipole matrix element between the ground and the excited state.

Due to the large Zeeman shift, the σ^--polarized beam does not fulfil the Raman condition and thus its susceptibility can be described by the two-level atom. As can be seen in figure 3, one has to sum over the susceptibilities of all four independent two-level systems, that can interact with the beam. Due to the large detuning from resonance, absorption can be neglected (<0.04% in our system), but the phase shift can become considerable.

The susceptibility is then described by [12]

$$\chi^{(-)} = \sum_{j=1}^{4} \frac{|\mu_j|^2\varrho_j}{\hbar\epsilon_0}\frac{\Delta_j + \mathrm{i}\frac{\Gamma}{2}}{\left(\frac{\Gamma}{2}\right)^2 + \Delta_j^2}. \tag{3}$$

Here, ϱ_j are the populations in the respective ground states, μ_j are the dipole matrix elements and Δ_j are the detunings relative to the respective transition, while the decay rate Γ is the same for all of them. The detunings Δ_j also depend on the probe detuning δ. The electric output field is then given by

$$\begin{aligned}|E_{\text{out}}|^2 &= |E_{\text{out},\sigma^+} + E_{\text{out},\sigma^-}|^2 \\ &= |(1-a)E_0\exp\{\mathrm{i}\chi^{(+)}kl/2\} + aE_0\exp\{\mathrm{i}\phi\}\exp\{\mathrm{i}\chi^{(-)}kl/2\}|^2 \\ &= a^2\exp\{-\mathrm{Im}\,\chi^{(-)}kl\}E_0^2 + (1-a)^2\exp\{-\mathrm{Im}\,\chi^{(+)}kl\}E_0^2\end{aligned}$$

$$+ 2a(1-a)\exp\{-(\mathrm{Im}\,\chi^{(-)} + \mathrm{Im}\,\chi^{(+)})kl/2\}$$
$$\times \cos\{\phi + (\mathrm{Re}\,\chi^{(-)} - \mathrm{Re}\,\chi^{(+)})kl/2\}E_0^2. \tag{4}$$

It can be seen that the first two terms of the equation describe the usual behaviour, described the respective susceptibility, while the last term is responsible for the interference and results in the appearance of the dispersive properties of the medium.

Together with equations (1) and (2), this yields the total transmission through the medium via

$$T(\delta) = \frac{|E_{\mathrm{out}}|^2}{|E_{\mathrm{in}}|^2}. \tag{5}$$

Because we are probing the sample with relatively short pulses, the pulse length limits the minimal EIT bandwidth. The Gaussian pulses are defined as

$$I(t) = I_0 \exp\left\{-\frac{t^2}{\tau^2}\right\}. \tag{6}$$

To include this limitation, one has to evaluate the convolution integral over the Fourier transformed of the Gaussian pulse

$$F(\delta) = \int_{-\infty}^{+\infty} I(t)\exp\{I2\pi\delta t\}\,\mathrm{d}t = I_0\sqrt{\pi}\tau\exp\{-\pi^2\tau^2\delta^2\}, \tag{7}$$

which finally yields the transmission through the cloud

$$T_P(\delta) = \int_{-\infty}^{+\infty} T(\delta')F(\delta-\delta')\,\mathrm{d}\delta'. \tag{8}$$

Unfortunately, there is no analytic solution to this integral.

4. Experimental results

We have measured the EIT-resonance spectrum for three different lengths of the probe pulse: $\tau = 5\ \mu$s, $\tau = 20\ \mu$s and $\tau = 100\ \mu$s. Figure 4 shows the data of one measurement with a pulse length of 20 μs and a coupling laser Rabi frequency of 1200 kHz. It has been calculated from the intensity, which has been measured with a calibrated CCD camera. In this measurement, it can be seen that the signal contains an absorptive (the peak itself) as well as a dispersive (the asymmetry) part.

The value for the phase $\phi = 4.95$ as well as the value for the intensity admixture $a^2 = 8.7\%$ were obtained from the fits of all measurements. The curves of all measurements were fitted with equation (5) and then approximated as a Gaussian to retrieve the widths of the EIT resonance. Here, they yielded $\sigma = 100$ kHz, $\gamma = 8$ kHz and $\delta_0 = -7.27$ MHz for the frequency offset due to the quadratic Zeeman shift. The ground-state decay rate γ usually corresponds to collisions between the atoms as well as collisions with the background gas. The collision rate can usually be neglected, especially in case of large-coupling laser Rabi frequencies. But it can also correspond to a transient effect: for low-coupling laser Rabi frequencies, a steady state in the atomic population cannot be reached within the time of a short probe pulse. For longer pulses, the Rabi frequency would have to be further decreased to assure the same number of photons (which is limited by the number of atoms) and would lead to a further decrease in transparency. This effect shows the same empiric behaviour as the collisional loss of polaritons and leads to non-negligible values of γ. The data in figures 5 and 6 show the results of the measurements with the 5 μs and the 20 μs pulses. For large-coupling laser Rabi frequencies, the coupling laser broadens the line width, while for lower Rabi frequencies, the pulse length is the limiting factor.

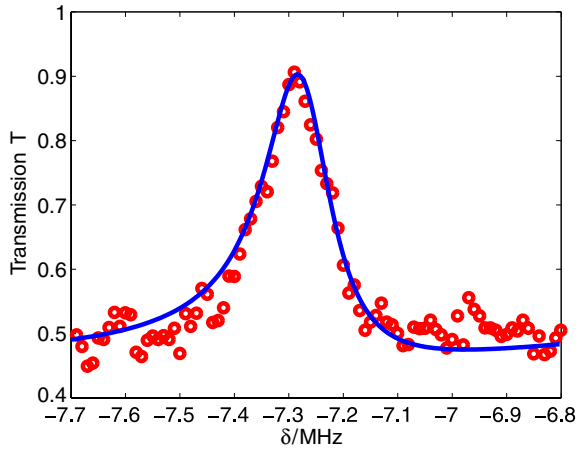

Figure 4. Transmission spectrum of a 20 μs pulse at a coupling laser Rabi frequency of 1200 kHz. The absorptive and dispersive parts in the signal can be recognized. The frequency offset of $\delta_0 = -7.27$ MHz corresponds to the differential quadratic Zeeman shift between the two ground state levels. This offset does not depend on the lasers and can thus be used to calibrate the magnetic offset field. For the fit, we used equation (5) as an approximation.

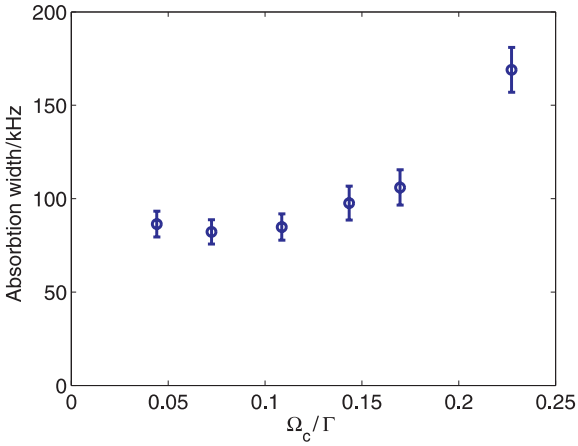

Figure 5. EIT measurement with 5 μs pulses. The figure shows the transparency width (Gaussian $1/e$ radius) depending on the Rabi frequency of the coupling laser. The probe pulses contain 3×10^5 photons within the size of the cloud, which correspond to a maximum Rabi frequency of 190 kHz. The error bars reflect the uncertainty in the phase ϕ.

The lack of sufficient coupling light results in an uncomplete transparency and limits the relative depth of the EIT dip in the signal. This can be seen in figure 7.

To obtain a very narrow line width, a measurement was made with 100 μs long pulses, containing 3.9×10^6 photons within the size of the cloud, which corresponds to a maximum Rabi frequency of 360 kHz. Figure 8 shows the result for a coupling laser Rabi frequency of 590 kHz. For lower values, the induced transparency was too low. Due to inefficient EIT, the absorptive part is so low that it is no longer visible. Instead, due to a large phase

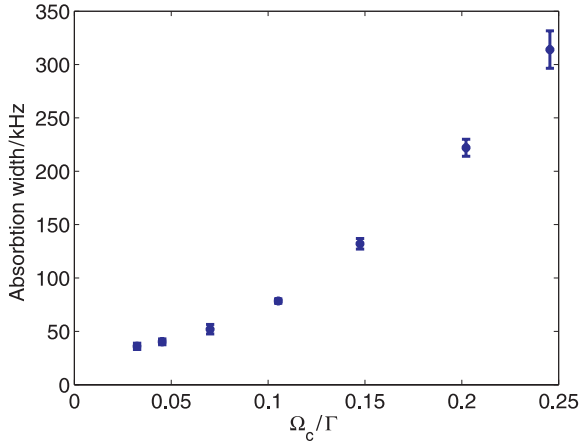

Figure 6. EIT measurement with 20 μs pulses. The figure shows the transparency width (Gaussian $1/e$ radius) depending on the Rabi frequency of the coupling laser. The pulses contain 2×10^6 photons within the size of the cloud, which correspond to a maximum Rabi frequency of 220 kHz. The width is much narrower than the one of the 5 μs pulses.

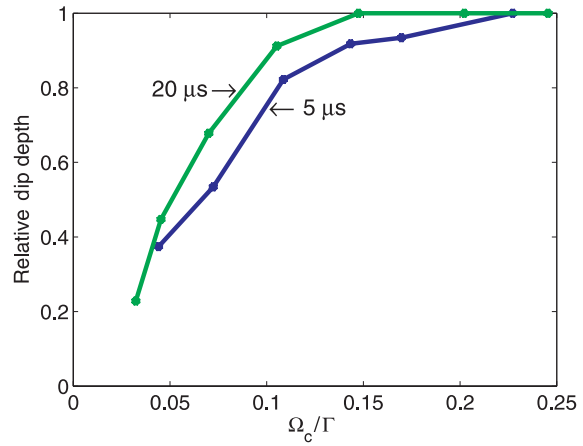

Figure 7. EIT measurement with 5 μs and the 20 μs pulses. The figure shows the relative depth of the EIT dip depending on the Rabi frequency of the coupling laser. The decrease for small Rabi frequencies corresponds to the transient effect that a steady state cannot be reached here within the time of a short probe pulse.

shift, the dispersive part of the signal gets enhanced compared to the measurements shown before.

To enhance the dispersive effect, the σ^--intensity admixture a^2 was increased to 25%, which also resulted in a different differential phase shift $\phi = 4.1$. With a Gaussian $1/e$-half width of 4 kHz, this is to our knowledge the narrowest EIT signal measured in ultracold atoms [13, 14]. Narrower signals of ∼30 Hz have been measured in buffer gas cells, where the buffer gas reduces the rate of bad collisions. Here, one is not limited by pulse lengths [15, 16].

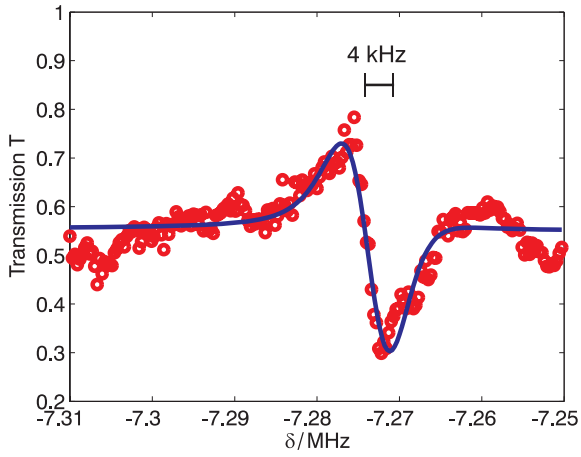

Figure 8. EIT measurement with a 100 μs pulse: the line width was reduced to 4 kHz. The transparency is so low that only the dispersive part of the signal can be recognized.

5. Conclusion and outlook

We have shown results on measuring electromagnetically induced transparency (EIT) in pure optically trapped rubidium atoms. The signals yield absorptive and dispersive properties of the atomic medium at the same time. Furthermore, we have measured the narrowest EIT line width in ultracold atoms.

This experiment is an important step towards polarization-dependent long-time storage of quantum information in an atomic cloud and the investigation of trapped dark-state polaritons.

In our measurements, we are still limited by the relatively low optical density of 0.76. The next step will be to optimize the cooling schemes and therefore increase the optical density. This will result in an enhanced atom–light interaction, required for better quantum information processing experiments. Furthermore, a higher optical density allows for a higher signal-to-noise ratio and thus for faster measurements.

Acknowledgments

We gratefully acknowledge the support of the Alexander von Humboldt foundation, the Landesstiftung Baden-Württemberg and the SFB/TR21.

References

[1] Harris S E, Field J E and Imamoğlu A 1990 *Phys. Rev. Lett.* **64** 1107
[2] Fleischhauer M and Lukin M D 2000 *Phys. Rev. Lett.* **84** 5094
[3] Karpa L and Weitz M 2006 *Nature Phys.* **2** 332
[4] Knill E, Laflamme R and Milburn G J 2001 *Nature* **109** 46
[5] Liu C, Dutton Z, Behroozi C H and Hau L V 2001 *Nature* **409** 490
[6] Phillips D F, Fleischhauer A, Mair A, Walsworth R L and Lukin M D 2001 *Phys. Rev. Lett.* **86** 783
[7] Bigelow M S, Lepeshkin N N and Boyd R W 2003 *Science* **301** 200
[8] Duan L-M, Lukin M D, Cirac J I and Zoller P 2001 *Nature* **414** 413
[9] Purves G T, Adams C S and Hughes I G 2006 *Phys. Rev.* A **74** 023805
[10] Xiao M, Li Y-q, Jin S-z and Gea-Banacloche J 1995 *Phys. Rev. Lett.* **74** 666

[11] Fleischhauer M, Imamoglu A and Marangos J P 2005 *Rev. Mod. Phys.* **77** 633
[12] Suter D 1997 *The Physics of Laser-Atom Interactions* (Cambridge: Cambridge University Press)
[13] Hau L V, Harris S E, Dutton Z and Behroozi C H 1999 *Nature* **397** 594
[14] Braje D A, Balic V, Goda S, Yin G Y and Harris S E 2004 *Phys. Rev. Lett.* **93** 183601
[15] Brandt S, Nagel A, Wynands R and Meschede D 1997 *Phys. Rev.* A **56** R1063
[16] Erhard M, Nußmann S and Helm H 2000 *Phys. Rev.* A **62** 061802